Batch to Continuous Photocatalytic Degradation of Phenol using TiO_2 and Au-Pd nanoparticles supported on TiO_2

Moses T. Yilleng, [‡†§] Emmanuel C. Gimba,[†] George I. Ndukwe,[†] Idris M. Bugaje,[§] David W. Rooney[‡] and Haresh G. Manyar*[,‡]

[‡] Theoretical and Applied Catalysis Research Cluster, School of Chemistry and Chemical Engineering, Queen's University Belfast, David-Keir Building, Stranmillis Road, Belfast, BT9 5AG, UK

[†]Department of Chemistry, Ahmadu Bello University, Zaria Nigeria

[§]National Research Institute for chemical Technology, Zaria Nigeria

*Corresponding Author

Haresh G. Manyar

Email: h.manyar@qub.ac.uk

Phone: +442890976608

Fax: + 44 28 90 974687

KEY WORDS: Visible light photocatalyst, Au/TiO_2, Pd/TiO_2, Continuous Taylor flow reactor, Photocatalytic degradation, Phenol

ABSTRACT: A series of Au-Pd/TiO_2 catalysts were synthesized in different weight % using sol-immobilization method. Of the range studied 1%Pd/TiO_2 catalyst achieved 86.4% conversion of phenol to CO_2 in a standard batch-slurry system utilizing UV. However under recycle or continuous operation Pd leaching from catalyst surface led to gradual deactivation. Au-Pd nanoparticles supported on TiO_2 P25 were stable and recyclable, here Au species were found to help to anchor Pd species on TiO_2, and no observable Pd leaching occurred. Utilizing UV, 1%Pd/TiO_2 showed faster rate of phenol degradation in comparison to Au-Pd/TiO_2, while 1%Au/TiO_2 and 0.5%Au-0.5%Pd/TiO_2 showed faster phenol degradation rates under visible light. The TiO_2 P25 support was also found to be active, stable and recyclable in phenol degradation utilizing UV; and was hence considered suitable for continuous operation. However poor oxygen mass transfer led to the formation and lay-down of polymeric species when using a Trickle bed approach. Operation in the Taylor flow regime was demonstrated to increase oxygen saturation and significantly reduced deactivation. Hence continuous photocatalytic degradation of phenol could be achieved using TiO_2 under Taylor Flow conditions.

1. Introduction

The synergistic and promotional effect of Au in Au-Pd catalysts has been widely reported in the past decade [1-4]. Within these studies, the superior activities of Au–Pd bimetallic catalysts, than monometallic Pd or Au catalysts, have been attributed to both ligand and ensemble effects [5,6]. It is considered that noble metals supported on TiO_2 surface promote the space-charge separation of photo-excited electron-hole pairs and suppress the charge recombination, resulting

in longer life-time of holes in TiO_2 valence band, thus enhancing the photocatalytic activity of TiO_2. Recently, the photocatalytic degradation of phenolics using Au-Pd based catalysts has received considerable attention [7,8]. Su et al. showed enhancement of photocatalytic activity of Au-Pd/TiO_2 catalysts over pristine TiO_2, wherein the metal nanoparticles are strongly involved in the reaction mechanism by suppressing undesired redox reactions. In photocatalysis, TiO_2 is the most prominent catalyst used in oxidation processes as it promotes the production of hydroxyl radicals which, through charge transfer and secondary radical formation processes, lead to the oxidation/reduction of organics in aqueous systems. TiO_2's ability to oxidize organic compounds under UV has led to such materials being applied in waste/contaminated water treatments.

Photocatalytic oxidation of phenolics utilizing UV is affected by solution concentration, pH, quantity, morphology and nature of the metal oxides present in the catalyst [9-12]. Besides, these factors, the reactor design must be optimized in order to assure complete degradation of organics [13]. Scaling up photocatalytic reactors is, however, a complex process with many factors needing consideration to yield a technically and economically viable process. These factors include distribution of pollutant and photocatalyst, pollutant/oxygen mass transfer, reaction kinetics, and irradiation characteristics [14].

While the current literature focuses on slurry systems using gas sparging and continuous mixing; these can lead to down-stream problems in the catalyst recovery and filtration stages. Within industry fixed bed multi-phase reactors e.g. trickle beds, are often used to mitigate this catalyst separation problem however given the large bed diameters illumination can be problematic when considering them for photocatalysis [15]. However small scale fixed bed reactors can be used for such processes. It is also known that multi-phase fixed bed reactors can

be operated under different gas and liquid flow regimes which in turn present different flow characteristics in the bed. Trickle flow is associated with a continuous co/counter-current flow of both the liquid and gas through the bed. Alternatively in Taylor flow the liquid and gas flow as separate slugs. Depending on the demands of the catalyst either of these two flow regimes, or others available, could be the most suitable.

Herein, this paper reports the heterogeneous photocatalytic degradation of Phenol using two different reactor types (suspension/slurry batch, and fixed-bed) with the latter operating in either trickle or Taylor flow) using Au-Pd/TiO_2 P25 and TiO_2 P25 catalysts. Such designs were used to develop a greater understanding of the processes involved and to enhance the availability of oxygen. Using such approaches the reactor can be continuously operated (herein for a period of three days).

2. Experimental Section

2.1. Materials

All reagents were of analytical grade. Palladium Chloride, Gold Tetrachloroaurate, Poly Vinyl Alcohol (MW = 10,000; 80% hydrolyzed) and methanol (HPLC grade) were obtained from Sigma Aldrich UK, TiO_2 P25 was obtained from Degussa (Evonik). Oxygen gas (99.5% Purity) was obtained from BOC UK.

2.2. Preparation of Au/TiO_2, Pd/TiO_2 and Au-Pd/TiO_2 catalysts

The metal nanoparticles (Au, Pd, Au-Pd) supported on TiO_2 catalysts were prepared by using a modified sol immobilization method reported by Su et al [8]. To an aqueous $PdCl_2$ and $HAuCl_4$ solution, 1 wt% PVA solution was added as a protective ligand [PVA/(Au & Pd) w/w = 1.2]. A freshly prepared 0.1 M $NaBH_4$ solution [$NaBH_4$/(Au&Pd) (mol/mol) = 5] was then added to

form a dark brown sol. After 30 min, the colloid was immobilized by adding TiO_2 (acidified to pH 1-2 by sulfuric acid) under vigorous stirring for 2 h. The catalyst was filtered, washed with distilled deionised water, dried at 120 °C overnight and calcined in air for 4hrs at 500 °C.

2.3. Characterization

UV–Vis absorption spectra were recorded using Perkin Elmer Lambda 6505 spectrophotometer in the range of 250-800 nm at a scanning speed of 300nm min^{-1}. Structural characterization was performed using X-ray diffraction measurements using Cu K_α radiation (1.5405 Å) on a PANalytical X'PERT PRO MPD diffractometer equipped with reflection geometry, a NaI scintillation counter, a curved graphite crystal monochromator and a nickel filter. The scattered intensities were collected from 5° to 80° (2θ) by scanning at 0.017° (2θ) steps with a counting time of 0.5 s at each step. The Au and Pd content of the fresh and used catalysts was determined by ICP-OES metal analysis using Perkin- Elmer, P-1000 Spectrometer. The surface area, total pore volume and average pore diameter were measured by N_2 sorption isotherms at 77K using Micromeritics ASAP 2020.

2.4. Measurement of photocatalytic activity

Photocatalytic activity was evaluated using phenol degradation. The reactors used were closed Pyrex reactors with a diameter of 42.7 mm and a height of 210 mm. 100 mL of a solution containing 94.11 mg/L (1mMol) of phenol in deionized water and 0.3 g of the catalyst was added to the reactor. The pH of the aqueous phenol solution was monitored during the reaction. The suspension was stirred at 650 rpm at ambient temperature for 2 hrs in the dark, and an aliquot was withdrawn to analyze equilibrium phenol concentration. The mixture was then exposed to UV light using a Rayonet RMR-600 reactor equipped with 6 (8 Watt) UV lamps (350nm wavelength), with an arc length of 76.2mm each. (**Figure S1**, supporting information). An

oxygen balloon was connected to the reactor in order to assure a high oxygen saturation of the solution. At regular time intervals aliquots were withdrawn for HPLC analysis.

Photocatalytic activity of the prepared catalysts was also evaluated using a tubular trickle bed column reactor. Typical reactor set up to operate under the Taylor flow regime, is shown in **Figure 1**. This reactor consisted of a quartz glass tube having an external diameter of 6mm and an internal diameter of 4 mm. Reagents were pumped to the reactor bed at a flow rate of 3ml min^{-1}. A second peristaltic pump connected to the phenol solution reservoir pumped fresh solution into the reservoir at a flow rate of 0.083ml min^{-1}. Using this approach the reactor operated continuously in a recycle mode i.e. recirculation of the reagents to the reactor with continuous make up of fresh reagent. In each experiment a batch of 300 mL containing 94.1 mg/L (1mMol) phenol in water was treated over a period of 92 hours. 1.0 g of a Pd, Au, and Pd-Au/TiO_2 was pelletized and sieved to the 456-600μm size range. At regular time intervals, aliquotes were withdrawn for HPLC analysis. HPLC analysis was performed using Agilent 1100 system equipped with Eclipse XDB-C18 reverse phase column (3.5μm, 4.6×150mm) and Diode Array Detector (DAD) at a wavelength of 254nm using 50% methanol and 50% water as the mobile phase.

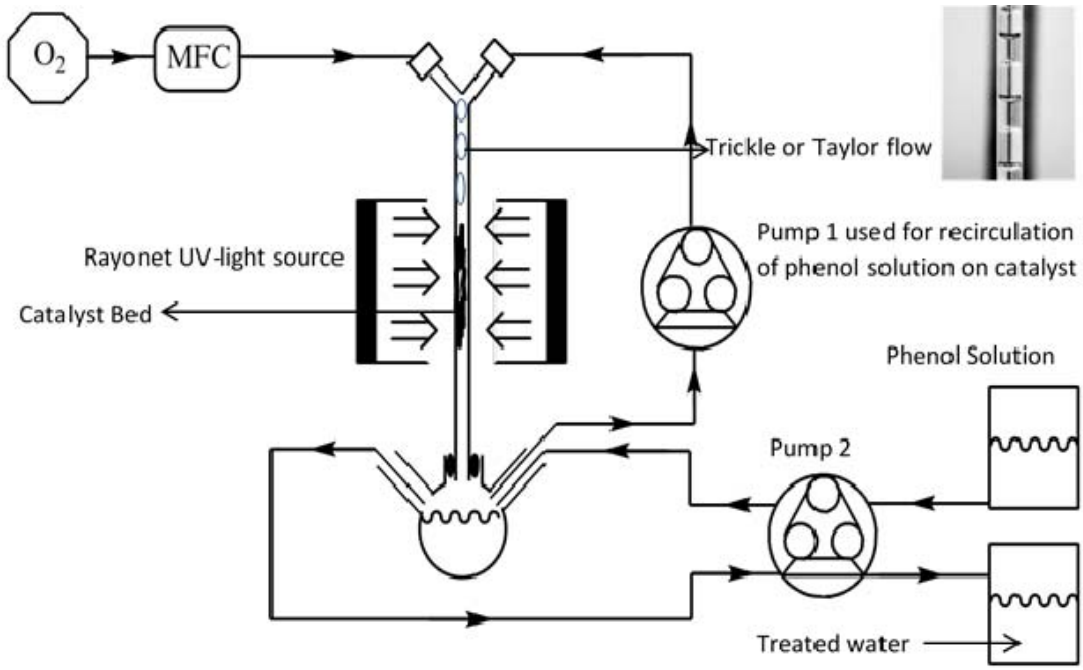

Figure 1. Schematic Diagram of the Taylor flow reactor system.

3. Results And Discussion

3.1. Catalyst characterization

The phase structure, crystallite size, and crystallinity of TiO_2 play an important role in photocatalytic activity, with many studies confirming that the anatase phase of TiO_2 shows higher photocatalytic activity than brookite or rutile phase [16]. The XRD patterns of Au-Pd/TiO_2 P25 catalysts calcined at 120 °C for 24 hours are shown in **Figure S2** (supporting information). The SEM and TEM images of Au-Pd/TiO_2 P25 catalysts are shown in **Figure S6**. The figure shows typical surfaces of doped TiO2 (Degussa P25). The TEM images showed metal nanoparticles were highly dispersed with some regions of TiO_2 doped with metals and some without doping. The EDS mapping (Figure S7) showed uniform metal dispersion over the surface of TiO_2.

The average crystal size of the TiO_2 was found to be a mixture of anatase crystallites (22.3 nm) and rutile crystallites (34.1 nm) as shown in **Table 1**. There were no peaks that indicate the presence of the metal nanoparticles or their metal oxides, which indicates high metal dispersion with the size of the metals nanoparticles below the detection limit of ~4nm [14]. In case of the bimetallic Au-Pd/TiO_2 catalysts, the nanoparticles are more likely to be individual metals than the metal alloys.

Table 1.

The physico-chemical properties of Au-Pd nanoparticles supported on TiO_2

Catalyst	BET surface area (m^2g^{-1})	Pore volume (cm^3g^{-1})	Crystallite size*		Band Gap** (eV)
			Anatase	Rutile	
1%Au/TiO_2	43.6	0.10	22.3	31.6	3.01
0.75%Au-0.25%Pd/TiO_2	44.8	0.12	22.2	34.2	2.97
0.5%Au-0.5%Pd/TiO_2	45.8	0.14	22.4	35.3	2.99
0.25Au%-0.75Pd/TiO_2	48.8	0.15	21.9	34.7	2.97
0.5%Pd/TiO_2	47.1	0.13	22.9	34.6	2.97
1%Pd/TiO_2	49.8	0.10	22.2	32.8	2.98
TiO_2 P25 Degussa	55.0	0.19	15.6	19.9	3.12

*Crystallite size was calculated using Scherrer equation, $\mathbf{D = K\lambda/\beta Cos\theta}$, **Band gap energies were calculated using the formula, $\boldsymbol{E = (h*c)/\lambda}$, *w*here; *h*= Planck constant (6.63×10^{-34} J s^{-1}), λ=cut off wavelength from the % reflectance graph, *c*= speed of light in vacuum ($\approx3\times10^{8}$ m s^{-1}), and 1eV = 1.6×10^{-19} J.

The surface area and pore volumes of the catalysts obtained by BET N_2 isotherm are shown in **Table 1**. As expected, the results show a decrease in the surface area of the catalyst after metal deposition. From the Diffuse Reflectance UV-Vis spectra (**Figure 2)** an absorption peak, with a maximum at 580 nm was observed for the 1wt%Au/TiO_2. This is attributed to the surface Plasmon resonance of spatially confined electrons in the 1.0wt% Au/TiO_2 catalyst. There are also band gap excitations in the region near 400 nm in all the spectra taken. The absorbance of the Au-Pd/TiO_2 catalysts varied with the content of Au in TiO_2; which could be attributed to the charge-transfer transition between the d electrons of the dopant and the Conduction Band (CB) or Valance Band (VB) of TiO_2 [18-20]. Based on the position of their absorbance maximum (**Figure S3**, supporting information), the band gap values of TiO_2 P25, Au, Pd and Au-Pd/TiO_2 P25 were calculated and are shown in the **Table 1**. It was observed that the Au-Pd/TiO_2 catalysts showed stronger visible light absorption than pristine TiO_2 P25, suggesting a greater potential for photocatalytic activity in the visible light to enhance the photodegradation of phenolics under natural sunlight.

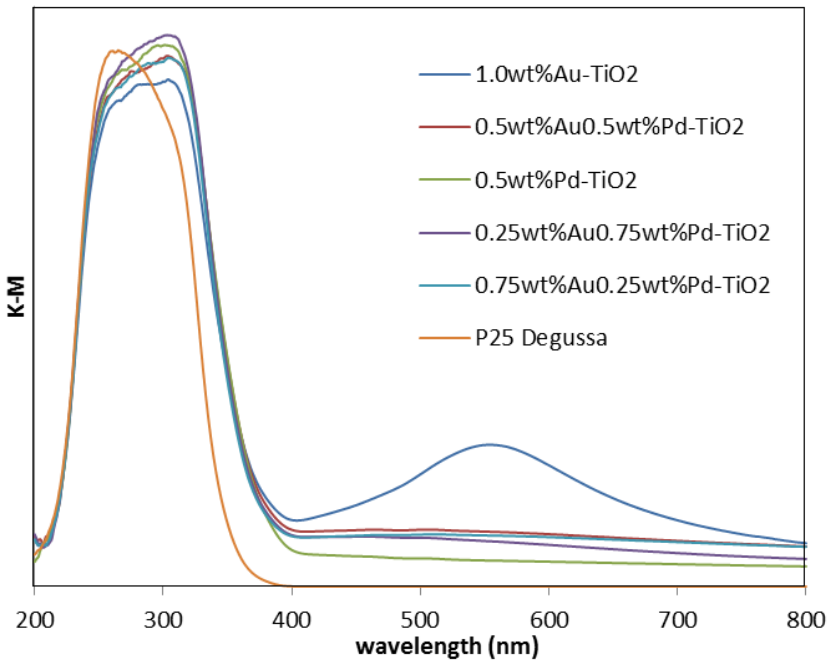

Figure 2. The DR UV-Vis spectra of Au-Pd nanoparticles supported on TiO_2 P25.

3.2. Photocatalytic degradation of phenol using batch reactor

The plot of total concentration of phenol as a function of time using UV irradiation is given in **Figure 3**. From the comparison of Au-Pd and Pd supported catalysts with TiO_2 P25, 1% Pd/TiO_2 showed the highest phenol degradation rate with 86.4% conversion of Phenol to CO_2 and H_2O after 120 min with O_2 whereas the 0.5%Pd/TiO_2 gives 79.7% and 1% Au/TiO_2 gives 73.4% conversion. For 0.5%Au0.5%Pd/TiO_2, 0.25%Pd0.75%Au/TiO_2 and 0.25%Au0.75Pd%/TiO_2 the % conversion of phenol is 69.0%, 64.4% and 41.8% respectively which are all lower than the monometallic catalysts. In contrast, 64.5% degradation is obtained with unmodified TiO_2 P25.

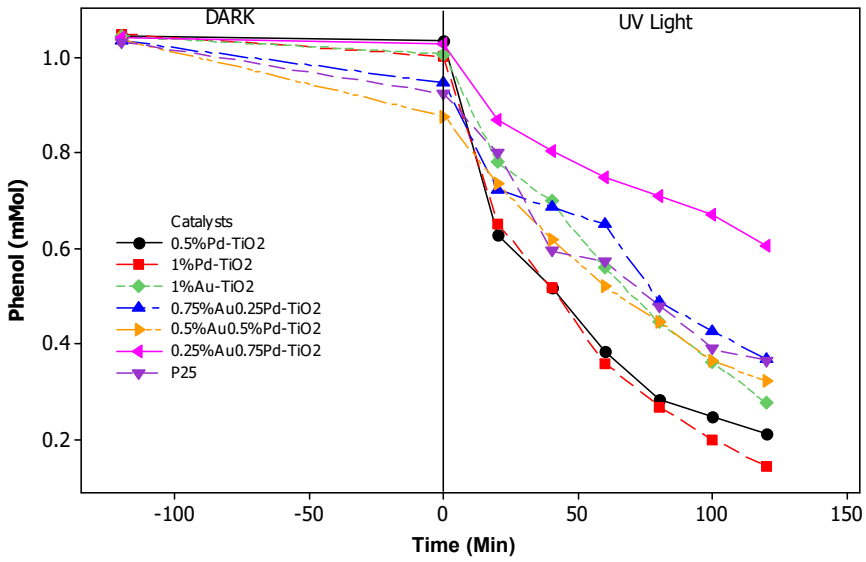

Figure 3. Photocatalytic degradation of phenol in UV using O_2 in the slurry type batch reactor.

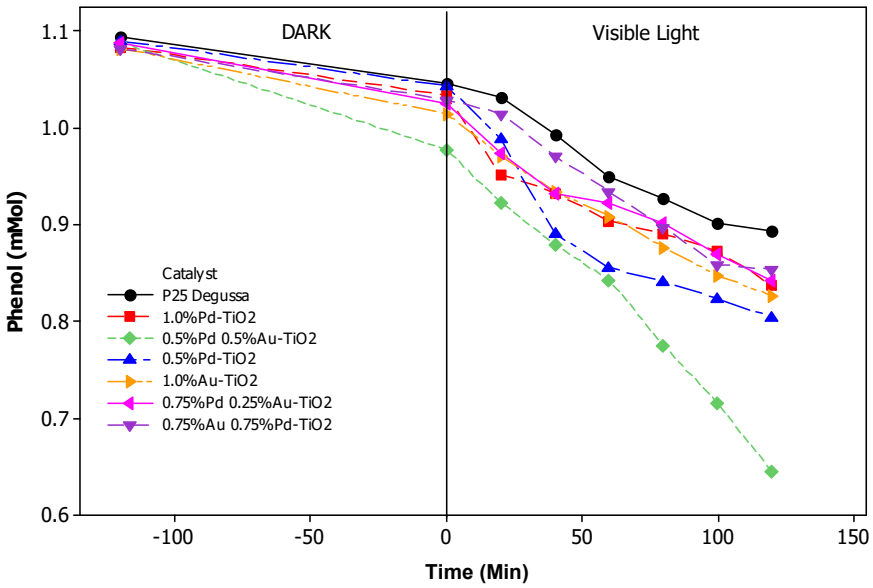

Figure 4. Photocatalytic degradation of phenol in the visible light (555 nm) using O_2 in the slurry type batch reactor.

From the dark results, although 2-10% of phenol adsorption was observed, but there was no direct correlation between adsorbed phenol concentration with phenol degradation rate, it could

be rather complicated due to several simultaneous effects including excitation of Au electrons to the conduction band of TiO_2 under UV irradiation causing detrimental effect on space-charge separation of electron-hole pairs [21-22].

Utilizing UV, 1%Pd/TiO_2 showed faster reaction rate for phenol degradation than Au-Pd/TiO_2 catalyst, while 1%Au/TiO_2 and 0.5%Au-0.5%Pd/TiO_2 showed faster phenol degradation rates under visible light (**Figure 4**). The synergetic effect of Au-Pd/TiO_2 showed highly enhanced activity for phenol degradation in the visible light region which is similar to other reports attributed to localized surface plasmonic effect and localized heating effect upon irradiation with visible light [23].

The Photocatalytic degradation of phenolics is often determined by using pseudo-first order kinetics [24-26]. The initial rate of Phenol Photocatalytic degradation was determined after the first 20min of the reaction by assuming Pseudo-first order kinetics with respect to the concentration of the bulk solution of phenol.

$$r = \frac{dC}{dt} = k_{obs}C \qquad \text{(eq. 1)}$$

Integrating the equation with the following restriction C= C_0 at t= 0, with C_0 being the initial concentration of the phenol solution and t the reaction time yields the following expression:

$$\ln\left(\frac{C_0}{C}\right) = -k_{obs}t \qquad \text{(eq. 2)}$$

The expression k_{obs} is the apparent pseudo-first-order rate constant and is affected by the concentration of phenol. The plot of -ln(C_0/C) versus time for phenol degradation using the slurry batch reactor in O_2 with the different modified photo catalyst in UV light is shown in **Figure 5** and the phenol degradation rates obtained with each catalyst are shown in **Table 2**.

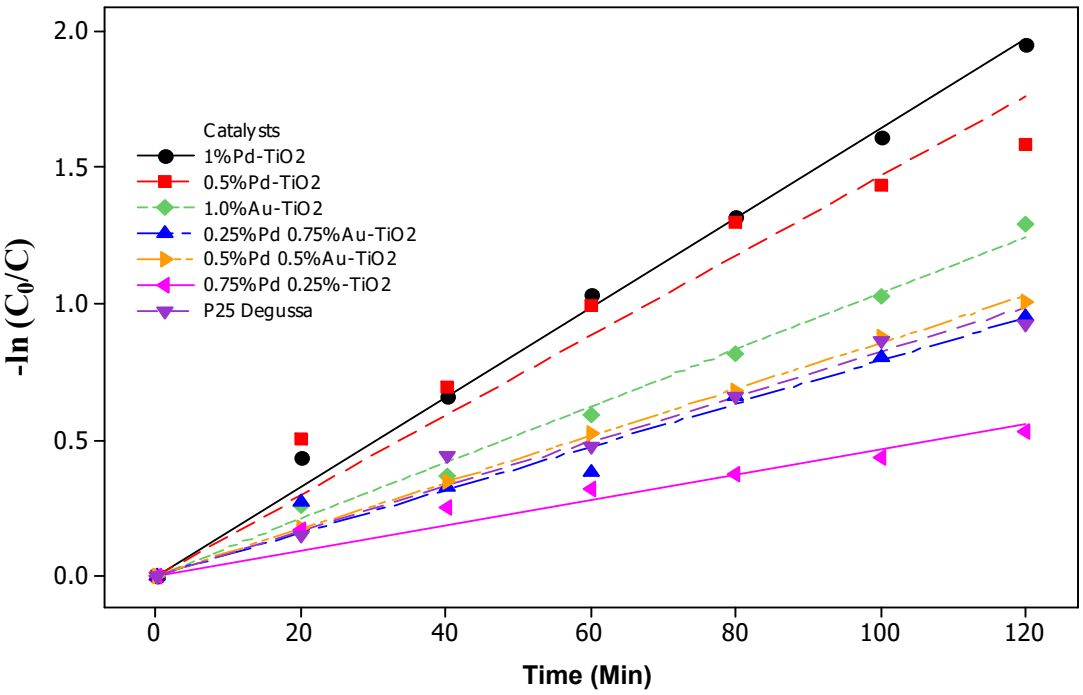

Figure 5. Pseudo-first order kinetics of photocatalytic degradation of phenol in O_2 using the slurry type batch reactor.

Table 2.

Pseudo-first order kinetic constants for the photocatalytic degradation of Phenol

Catalyst	Rate Constant k_{phenol} (min^{-1})
TiO_2 P25	0.0047
1wt%Au/TiO_2	0.0055
0.75wt%Au-0.25wt%Pd/TiO_2	0.0039
0.5wt%Au-0.5wt%Pd/TiO_2	0.0046
0.25wtAu-0.75wt%Pd/TiO_2	0.0025
0.5wt%Pd/TiO_2	0.0056
1wt%Pd/TiO_2	0.0058

3.3. The effect of catalyst loading on photocatalysis

To determine the optimal catalyst loading, a set of experiments with varying catalyst mass in the range 0.1-0.4 g using 0.5wt%Pd/TiO_2 as catalyst was studied at pH 6.4 over 80min (**Figure 6**). An increase in the amount of catalyst provides an increased number of active sites for adsorption; however, this also causes a simultaneous increase in solution opacity which further causes a decrease in the penetration of UV light. This suggests that the amount of photo-catalyst to be used should maintain a balance between these two opposing effects [27-30]. For this study, clearly the photocatalytic degradation for phenol increases as the catalyst loading is increased from 0.1g to 0.3g but when the catalyst loading is increased further to 0.4g, the amount adsorbed in the first 20min increased while the rate of degradation decreases after 40min. These show that the optimum catalyst loading to be used is 0.3g in 100ml of the phenol solution.

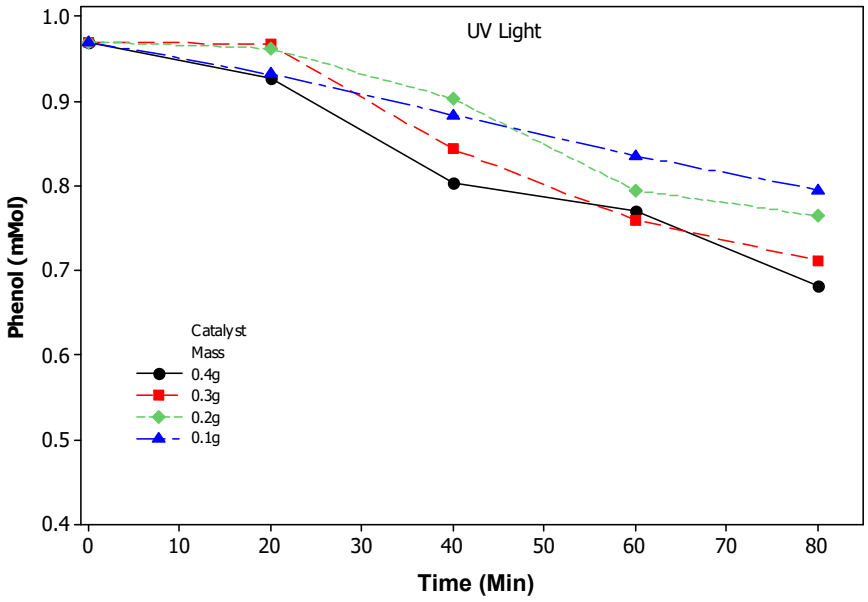

Figure 6. Effect of catalyst loading on the Photocatalytic degradation of Phenol with 0.5wt%Pd/TiO_2 in O_2.

HPLC analysis suggests that the polymerization of phenol and formation of intermediates like catechol, Pyrogallol and Benzoquinone occurred immediately after the first 20mins of irradiation with UV light. This was evident from the brownish colors formed which slowly disappeared. The results of HPLC analysis indicated that the polymer was transformed to hydroxylated products that were the same as those intermediates produced in photocatalysis of phenol, and further oxidized via organic acids to CO_2 in the course of the photocatalytic degradation of Phenol [31].

3.4. Stability and reusability of the catalyst

To develop a continuous process, stability and reusability of any photocatalyst is critical to develop potential practical applications [32-33]. Post reaction, TiO_2 P25, 0.5wt%Pd/TiO_2 and 0.5%Pd-0.5%Au/TiO_2 catalysts were recovered by filtration, washed and dried and evaluated for reusability under the same experimental conditions (**Figure 7**). Significant loss in activity was

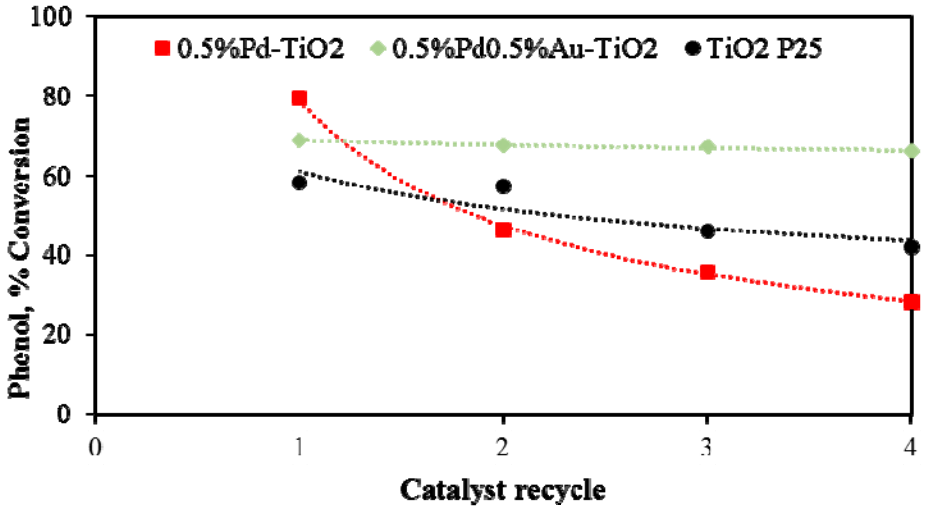

Figure 7. Catalyst reusability in the Photocatalytic degradation of Phenol.

Table 3.

The metal content of fresh and used Au-Pd/TiO_2 catalysts as determined by ICP-OES analysis

Catalyst	Fresh		Used catalyst	
	% Au	%Pd	% Au	% Pd
1wt%Au/TiO_2	1.02	-	0.96	-
0.75wt%Au-0.25wt%Pd/TiO_2	0.74	0.23	0.60	0.11
0.5wt%Au-0.5wt%Pd/TiO_2	0.46	0.40	0.46	0.39
0.25wtAu-0.75wt%Pd/TiO_2	0.21	0.72	0.19	0.68
0.5wt%Pd/TiO_2	-	0.43	-	0.33

observed for TiO_2 and monometallic Pd/TiO_2 catalysts which could be due to metal leaching as well as deposition of polymeric species on the catalysts surface. Besides metal leaching, the loss of activity could also be due to poisoning of the catalyst surface with intermediates. The Pd metal content of the fresh and used Pd/TiO_2 catalyst using ICP-OES analysis (**Table 3**) showed a clear decrease in Pd content on used catalyst due to metal leaching. However, Pd metal content for fresh and used 0.5%Au-0.5%Pd/TiO_2 and 0.25%Au-0.75%Pd/TiO_2 was pretty consistent within the experimental errors, which indicated that bimetallic Au-Pd catalysts were more stable to leaching in the photocatalytic conversion of Phenol to water. This was further supported by the reusability of recovered bimetallic Au-Pd catalysts.

3.5. Comparison of photo and thermal degradation of phenol in UV, Visible and dark regions

Comparing the amount of phenol converted using the visible light and the UV light (**Figure 8)**, it was shown that the bimetallic 0.5%Pd-0.5%Au/TiO_2 P25 catalyst was not only more stable to leaching but also had significantly enhanced Photocatalytic activity in visible light region. This could be attributed to their ability to suppress the recombination of the photogenerated electron-

hole pairs in the reaction. Interaction between Au-Pd helps to anchor Pd on TiO_2 more strongly thus suppressing the leaching of Pd. Also the 0.5%Au-0.5%Pd/TiO_2 catalyst showed remarkable ability to both adsorb and degrade phenol thermally in the dark region conversion, which can allow for continuous day and night operation in real life solar photodegradation of phenolics (**Figure 4**). The thermal catalytic efficiency of TiO_2 P25 was further compared with 0.5%Pd-0.5%Au/TiO_2 in terms of the rate of the reaction. Here the rate at which 0.5%Pd-0.5%Au/TiO_2 thermally degraded phenol in the absence of light is 2.0 times higher than the P25 under the same conditions.

0.5%Pd-0.5%Au/TiO_2 catalyst showed very stable catalytic activity over 4 recycles which was complimentary to metal content analysis of used catalyst, hence bimetallic Pd-Au/TiO_2 P25 could be the potential catalyst for continuous flow operation.

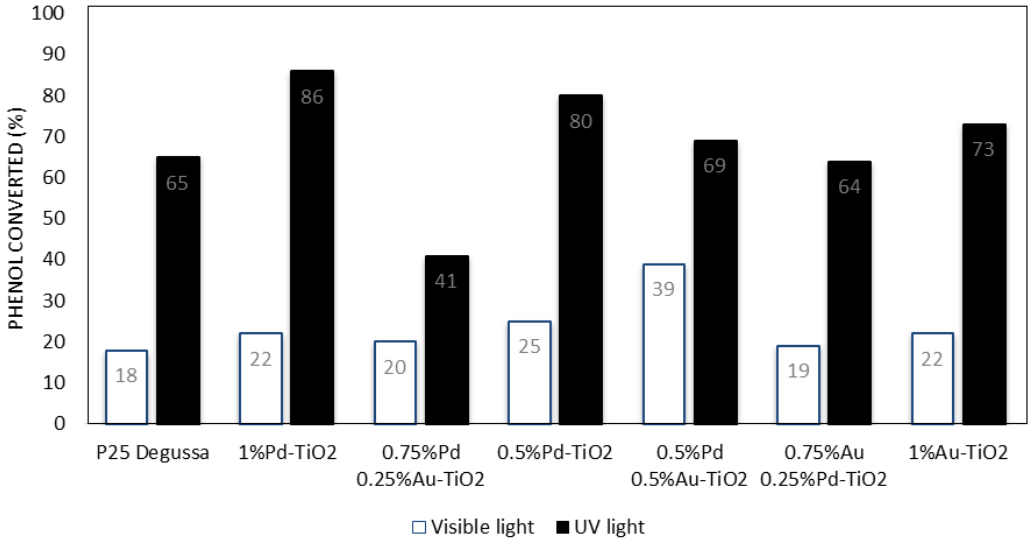

Figure 8. Comparison of Phenol, % Conversion using the Visible and UV light in O_2 in the slurry Batch reactor.

3.6. Photocatalytic degradation of phenol using continuous trickle-bed reactor

Photocatalytic degradation of phenol in continuous flow operation was studied using trickle bed reactor (**Figure 9**). Increase in the contact time between phenol and the catalyst in the presence of sufficient O_2 promoted the photodegradation of phenol to higher conversions. It was observed that the conversion of phenol to CO_2 and water is limited by the availability of oxidant in the reaction. Mass transfer limitations often occur in immobilized photocatalytic systems [34-35]. Photocatalytic degradation of phenol showed that the removal efficiency of the catalyst was 99.9% when TiO_2 P25 was used in the Trickle Bed reactor in the presence of hydrogen peroxide as the oxidant. While 71.9% conversion was achieved when TiO_2 P25 was used with O_2 and 70.3% when 0.5%Pd/TiO_2 was used under the same reaction conditions. These results indicated that rate of phenol degradation using Au-Pd/TiO_2 photocatalyst could be affected by the deposition of intermediates on the surface of the catalyst.

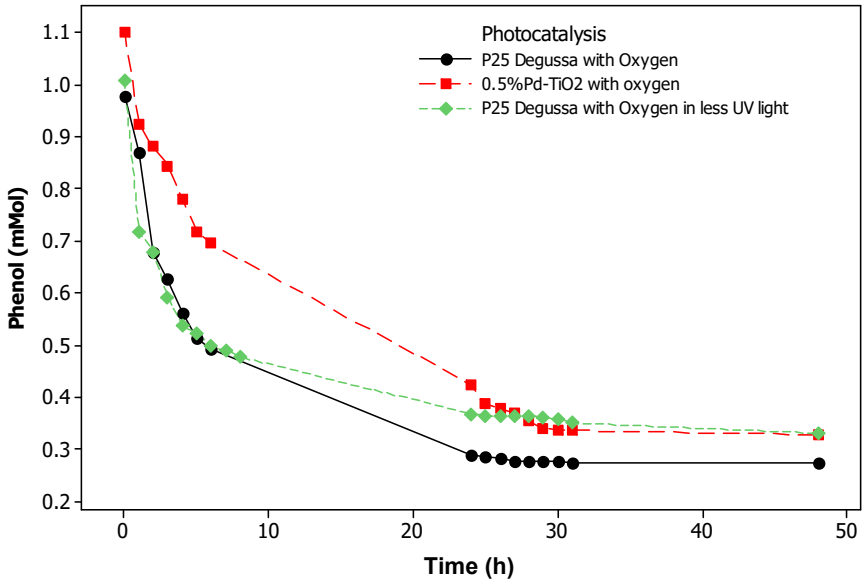

Figure 9. Photocatalytic degradation of phenol in O_2 using the Trickle Bed reactor.

To evaluate catalyst stability in continuous process, further tests were conducted using the fresh catalyst in the Trickle Bed reactor with O_2. In a control experiment with limiting the

intensity of UV-light, the formation of polymeric species on the surface of the catalyst during the reaction was noticed. In a separate experiment conducted by limiting O_2 and increased intensity of UV light, the deposition of species on the surface of the catalyst was again observed. As shown in **Figure S4** (supporting information), it is evident that the availability of O_2 is vital for the complete decomposition of intermediates species formed in the reaction. If the TiO_2 P25 catalyst has both sufficient oxygen and UV irradiation complete conversion of Phenol to CO_2 is evident through the catalyst retaining its original color. After the catalytic activity test, the used catalyst was analyzed using Temperature Program Oxidation (TPO). (**Figure S5**, supporting information). TPO of used catalyst from activity test performed by limiting O_2 showed that carbonic species formed were more difficult to remove and required higher temperatures. In order to optimize and properly design the regeneration of deactivated catalysts, knowledge of the carbonaceous burning kinetics is desirable [36]. The result of this analysis is also presented in **Table S1 (**supporting information) depicting the wt% of carbonaceous species on the catalyst.

3.7. Photocatalytic degradation of phenol using continuous Taylor flow reactor

The photocatalytic efficiency of the monometallic Pd and Au on TiO_2 catalyst can be enhanced by reducing the mass transfer resistance and increasing the availability of oxygen by using the Taylor flow reactor running gas liquid slugs, where O_2 replenishes the catalyst surface continually. Hence, the catalyst surface was not deactivated with carbonaceous deposits thereby increasing the stability and life-time of the catalyst under continuous mode [37-38]. For the 0.5%Pd-0.5%Au/TiO_2 over 76% phenol is converted and this is retained for 52 hrs (**Figure 10**). It should be noted that these trends continued over the 52 hr run. Furthermore the photo-response

of the 0.5%Pd-0.5%Au/TiO_2 in the visible light region, as discussed earlier, makes this a viable catalyst for industrial application in wastewater treatment.

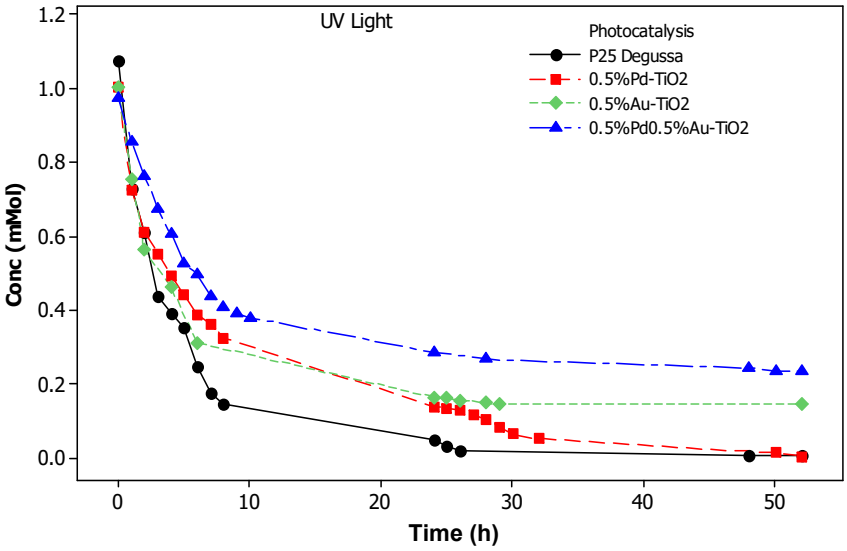

Figure 10. Photocatalytic degradation of phenol in O_2 using the Taylor flow reactor.

4. Conclusions

In present study, it was demonstrated that TiO_2 P25, Pd, Au and Au-Pd/TiO_2 monometallic and bimetallic catalysts show high photocatalytic activity under UV and Visible light illumination. Monometallic Pd supported catalysts gradually deactivate due to leaching of Pd, however Au-Pd/TiO_2 P25 suppresses Pd leaching and enhances photocatalytic activity. Photodegradation of phenolics is mass transfer limited with respect to availability of oxygen on the catalyst surface. It was observed that the combination of poor mass transfer and excess UV within the trickle bed reactor led to the formation of heavier hydrocarbon species and some deactivation of the catalyst. However this process could be significantly reduced by saturating the catalyst with O_2 and then providing a sufficient volume of solution in order to desorb any intermediates, effectively washing the catalyst. Such a process could be achieved using the alternating gas-

liquid slugs flow pattern produced in the Taylor flow reactor and showed stable continuous activity over the 52 hour operating window.

Acknowledgements

The authors gratefully acknowledge financial Support from the STEP-B of National Research Institute for Chemical Technology (NARICT), Zaria as well as the recent Collaboration between the Center for the theory and Application of Catalysis (CenTACat) and NARICT.

Supporting Information

Additional information on batch reactor scheme, XRD diffraction patterns, comparison of various catalysts for phenol conversions over time, catalyst bed photos in the trickle bed reactor, weight of carbonaceous materials can be found in the supporting information.

References

[1] G. Panzera, V. Modafferi, S. Candamano, A. Donato, F. Frusteri, P.L. Antonucci, CO selective oxidation on ceria-supported Au catalysts for fuel cell application, J. of power sources, 135, 1 (2004) 177-183.

[2] W. Hou, N. A. Dehm, R.W.J. Scott, Alcohol oxidations in aqueous solutions using Au, Pd, and bimetallic AuPd nanoparticle catalysts, J. of Catal., 253, 1 (2008**)** 22-27.

[3] G. Li, J. Edwards, A.F. Carley, G.J. Hutchings, Direct synthesis of hydrogen peroxide from H_2 and O_2 using zeolite-supported Au-Pd catalysts, Catal. Tod., 122 (2007) 361–364.

[4] C. Hamill, R. Burch, A. Goguet, D. Rooney, H. Driss, L. Petrov, M. Daous, Evaluation and mechanistic investigation of a AuPd alloy catalyst for the hydrocarbon selective catalytic reduction (HC-SCR) of NOx, Appl. Catal. B: Env., 147 (2014) 864-870.

[5] H.L. Abbott, A. Aumer, Y. Lei, C. Asokan, R.J. Meyer, M. Sterrer, S. Shaikhutdinov, H. Freund, CO Adsorption on Monometallic and Bimetallic Au-Pd Nanoparticles Supported on Oxide Thin Films, J. of P. Chem. C, 114, 40 (2010) 17099-17104.

[6] A. Mills; S.L. Hunte, An Overview of semiconductor photocatalysis, J. of Photochem. and Photobio. A: Chem., 108, 1 (1997) 1-35.

[7] M. Maicu, M.C. Hidalgo, G. Col'on, J.A. Nav'io, Comparative study of the photodeposition of Pt, Au and Pd on pre-sulphated TiO_2 for the photocatalytic decomposition of phenol, J. of Photochem. and Photobio. A: Chem., 217 (2011) 275-283.

[8] R. Su, R. Tiruvalam, Q. He, N. Dimitratos, L. Kesavan, C. Hammond, J.A. Lopez-Sanchez, R. Bechstein, C.J. Kiely, G.J. Hutchings, F. Besenbacher, Promotion of Phenol Photodecomposition over TiO_2 Using Au, Pd and Au-Pd Nanoparticles, ACS Nano, 6, 7 (2012) 6284-6292.

[9] A. Mills, R. H Davis, D. Worsley, Purification by Semiconductor Photocatalysis, Chem. Soc. Rev., 22 (1993) 419-425.

[10] K. R. Reddy, M. Hassan, V. G. Gomes, Hybrid nanostructures based on titanium dioxide for enhanced photocatalysis, Appl. Catal. A. Gen., 489 (2015), 1-16.

[11] K. R. Reddy, K. Nakata, T. Ochiai, T. Murakami, D. A. Tryk, A. Fujishima, Facile Fabrication and Photocatalytic Application of Ag Nanoparticles-TiO2 Nanofiber Composites, J. Nanosci. and Nanotech., 11, 4, (2011) 3692-3695.

[12] H. G. Manyar, P. Iliade, L. Bertinetti, S. Coluccia, G. Berlier, Structural and spectroscopic investigation of ZnS nanoparticles grown in quaternary reverse micelles, J. of Coll. and Inter. Sci., 354 (2011) 511-516.

[13] N.J. Peill, M.R. Hoffmann, Development and optimization of a TiO_2-coated fiber--optic cable reactor: photocatalytic degradation of 4-chlorophenol, Env. Sci. & Tech., 29, 12 (1995) 2974-2981.

[14] C. Mccullagh, N. Skillen, M. Adams, P.K.J. Robertson, Photocatalytic reactors for environmental remediation: a review, J. of Chem. Tech. and Biotech., 86, 8 (2011) 1002-1017.

[15] K. Mehrotra, G.S. Yablonsky, A.K. Ray, Kinetic studies of photocatalytic degradation in a TiO_2 slurry system: Distinguishing working regimes and determining rate dependences, Ind. & Eng. Chem. Res., 42, 11 (2003) 2273-2281.

[16] O. Carp, C.L. Huisman, A. Reller, Photoinduced reactivity of titanium dioxide, Prog. in Sol. St. Chem., 32, 1 (2004) 33-177.

[17] S. E. Wanke, P.C. Flynn, The sintering of supported metal catalysts, Catal. Rev., 12, 1 (1975) 93-135.

[18] L. Yang, G.H. Li, L.D. Zhang, Effects of surface resonance state on the Plasmon resonance absorption of Ag nanoparticles embedded in partially oxidized amorphous Si matrix., Appl. Phy. Lett., 76 (2000) 1537-1539.

[19] X. Chen, S.S. Mao, Titanium dioxide nanomaterials: synthesis, properties, modifications, and applications, Chem. Rev., 107, 7 (2007) 2891-2959.

[20] L. Kumaresan, B. Palanisamy, M. Palanichamy, V. Murugesan, The Syntheses, Characterizations, and Photocatalytic Activities of Silver, Platinum, and Gold Doped TiO_2 Nanoparticles, Env. Eng. Res., 16, 2 (2011) 81-90.

[21] M. Y. Seon, S. B. Rawal, J. E. Lee, J. Kim, H.-Y. Ryu, D.-W. Park, W. I. Lee, Size-dependence of plasmonic Au nanoparticles in photocatalytic behavior of Au/TiO_2 and $Au@SiO_2/TiO_2$, Appl. Catal. A: Gen., 499 (2015) 47-54.

[22] T. Tsukasa, I. Shigeyoshi, K. Susumu, Y. Hiroshi, Effects of adsorbents used as supports for titanium dioxide loading on photocatalytic degradation of propyzamide, Env. Sci. & Tech., 30, 4 (1996) 1275-1281.

[23] K. Masao, O. Ichiro, Eds., Photocatalysis: science and technology [M], Springer, Tokyo, (2003) 29-33.

[24] P. Xu, G. Zeng, D. Huang, L. Liu, C. Lai, M. Chen, C. Zhang, X. He, M. Lai, Y. He, Photocatalytic degradation of phenol by the heterogeneous Fe_3O_4 nanoparticles and oxalate complex system, RSC Advances, 4 (2014) 40828-40836.

[25] A. Hamza, J.T. Fatuase, S.M. Waziri, O.A. Ajayi, Solar Photocatalytic degradation of phenol using nanosized ZnO and α-Fe_2O_3, J. of Chem. Eng. and Mat. Sci., 4, 7 (2013) 87-92.

[26] R. Qiu, L. Song, Y. Mo, D. Zhang, E. Brewer, Visible light induced photocatalytic degradation of phenol by polymer- modified semiconductors: Study of the influencing factors and the kinetics, Reac. Kinet. and Catal. Lett., 94, 1 (2008) 183-189.

[27] K. Selvam, M. Muruganandam, I. Muthuvel, M. Swaminathan, The influence of inorganic oxidants and metal ions on semiconductor sensitized photodegradation of 4-flurophenol, Chem. Eng. J., 128 (2007) 51-57.

[28] R. Vinu, M. Girighar, Kinetics of Simultaneous Photocatalytic Degradation of Phenolic Compounds and Reduction of Metal Ions with Nano-TiO_2, Env. Sci. and Tech., 42 (2008) 913–919.

[29] A.A. Adesina, Industrial exploitation of photocatalysis: progress, perspectives and prospects, Catalysis surveys from Asia, 8, 4 (2004) 265-273.

[30] K.M. Parida, S. Parija, Photocatalytic degradation of phenol under solar radiation using microwave irradiated zinc oxide, Solar Energy, 80, 8 (2006) 1048-1054.

[31] H. Chun, W. Yizhong, T. Hongxiao, Destruction of phenol aqueous solution by photocatalysis or direct photolysis, Chemosphere, 41, 8 (2000) 1205-1209.

[32] W. Li, Y. Bai, C. Liu, Z. Yang, X. Feng, X. Lu, N. K. van Der Laak, K.-Y. Chan, Highly Thermal Stable and Highly Crystalline Anatase TiO_2 for Photocatalysis, Env. Sci. and Tech., 43 (2009) 5423–5428.

[33] Z.-Y. Ding, S. N.V.K. Aki, M. A. Abraham, Catatytic Supercritical Water Oxidation: Phenol Conversion Oxidation: Phenol Conversion, Env. Sci. and Tech., 29 (1995) 2748-2753.

[34] D.F. Ollis, E. Pelizzetti, N. Serpone, Photocatalyzed Destruction of water contaminants, Env. Sci. Tech., 25, 9 (1991) 1522-1529.

[35] A.K. Ray, A. ACM Beenackers, Novel swirl flow reactor for kinetic studies of semiconductor photocatalysis, AIChE J., 43, 10 (1997) 2571-2578.

[36] B. Sanchez, M.S. Gross, B.D. Costa, C.A. Querini, Coke analysis by temperature-programmed oxidation: Morphology characterization, Appl. Catal. A: Gen., 364 (2009) 35-41.

[37] B. P. Chaplin, M. Reinhard, W. F. Schneider, C. Schuth, J. R. Shapley, T. J. Strathmann, C. J. Werth, Critical Review of Pd-Based Catalytic Treatment of Priority Contaminants in Water, Env. Sci. and Tech., 46 (2012) 3655−3670.

[38] S.-K., Lee; A. Mills, Platinium and Palladium in semiconductor Photocatalytic systems, Platinum Metals Review, 47, 2 (2003) 61-72.

Supporting Information

Batch to Continuous Photocatalytic Degradation of Phenol using TiO_2 and Au-Pd nanoparticles supported on TiO_2

Moses T. Yilleng, [‡†§] Emmanuel C. Gimba,[†] George I. Ndukwe,[†] Idris M. Bugaje,[§] David W. Rooney[‡] and Haresh G. Manyar*[,‡]

[‡] Theoretical and Applied Catalysis Research Cluster, School of Chemistry and Chemical Engineering, Queen's University Belfast, David-Keir Building, Stranmillis Road, Belfast, BT9 5AG, UK

[†]Department of Chemistry, Ahmadu Bello University, Zaria Nigeria

[§]National Research Institute for chemical Technology, Zaria Nigeria

*Corresponding Author

Haresh G. Manyar
Email: h.manyar@qub.ac.uk
Phone: +442890976608
Fax: + 44 28 90 974687

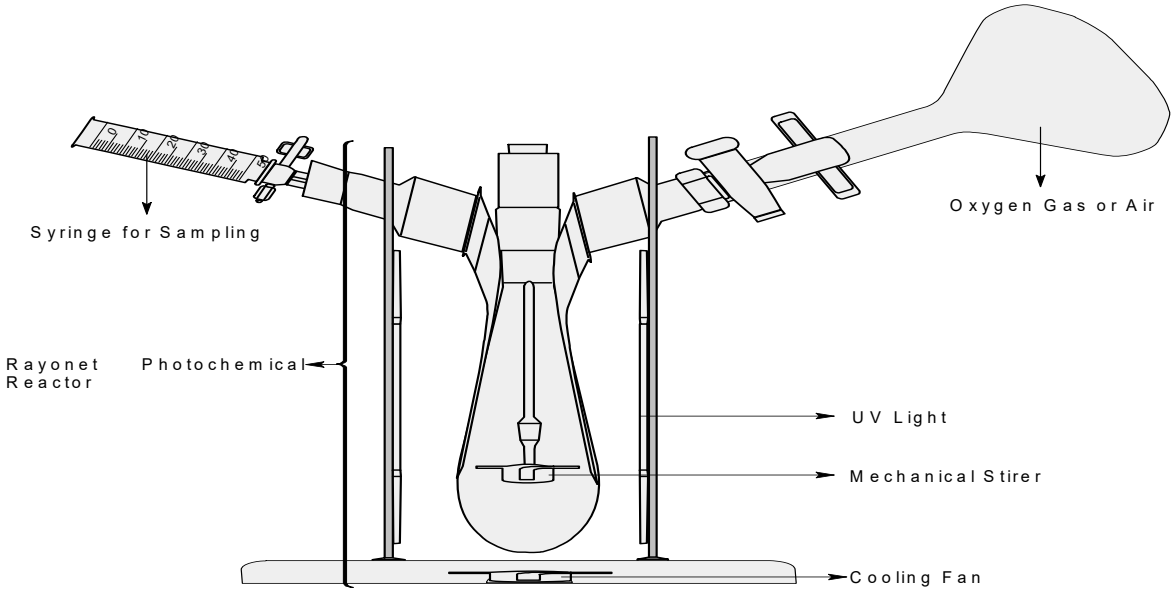

Figure S1. Diagram of the Slurry/Suspension Batch Setup using a Rayonet RMR-600 reactor.

The RMR-600 consists of a 279.4mm long square base and 266.7mm high (external measurements) chamber manufactured from Alzak aluminum. The reactor has 6 (8 Watt) UV lamps (350nm wavelength), with an arc length of 76.2mm each (48 lamp Watts total). The distance between the UV lamp and the surface of the solute was set at 63.5 mm.

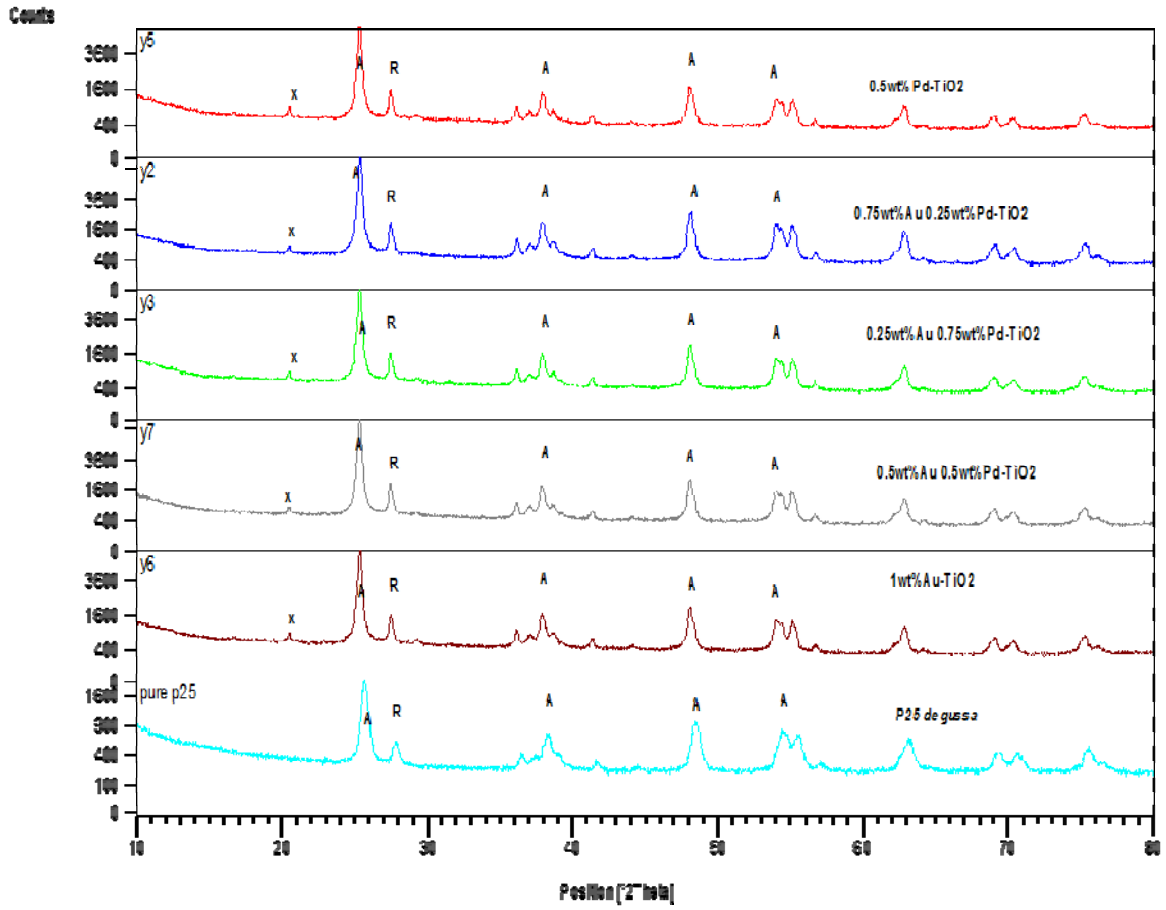

Figure S2. XRD Patterns of Au-Pd/TiO_2 Prepared by sol Immobilization, diffraction peaks corresponding to the (i) A-anatase phase and (ii) R-rutile phase.

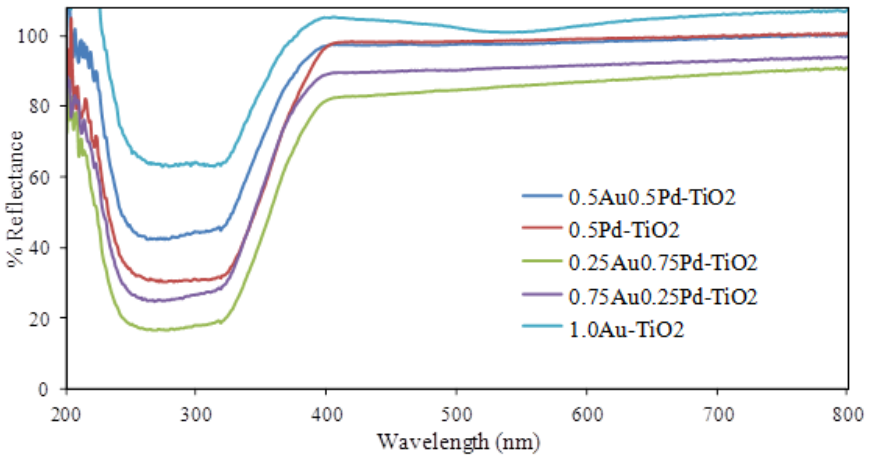

Figure S3. Diffuse Reflectance UV-Vis spectra of Au-Pd/TiO_2.

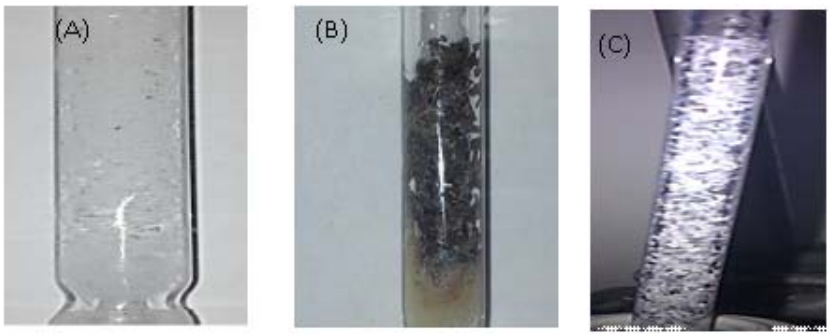

Figure S4. Picture of Catalyst Bed: (A) Fresh P25. (B) P25 with limited UV light in Trickle Bed (C) P25 in Oxygen with Taylor flow.

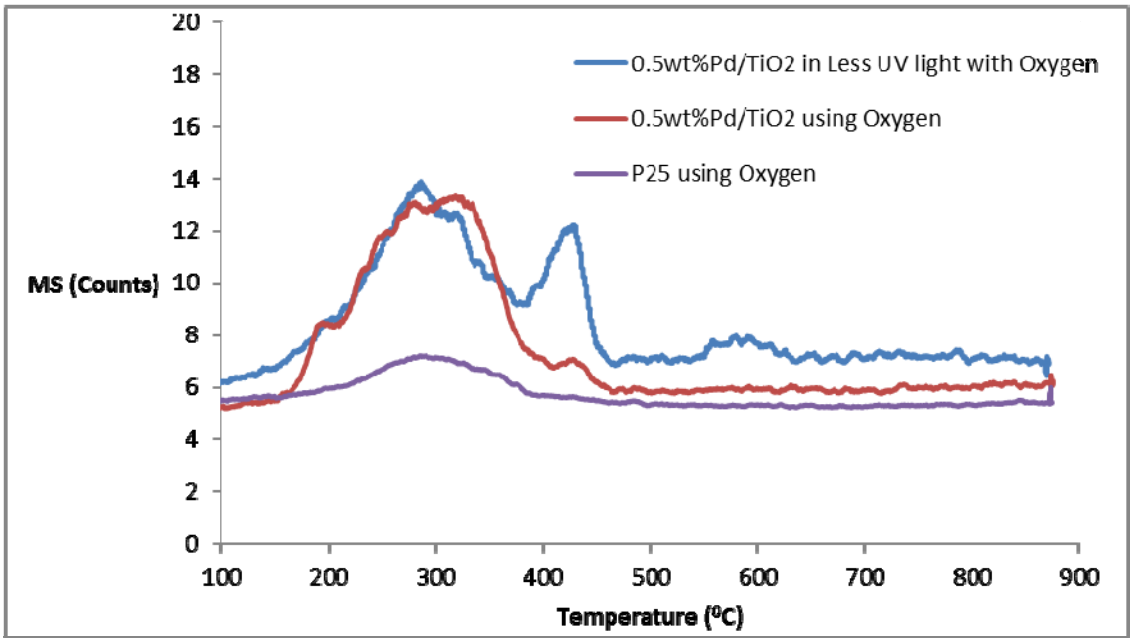

Figure S5. Temperature programmed oxidation of catalysts showing evolution of CO_2 as a function of temperature.

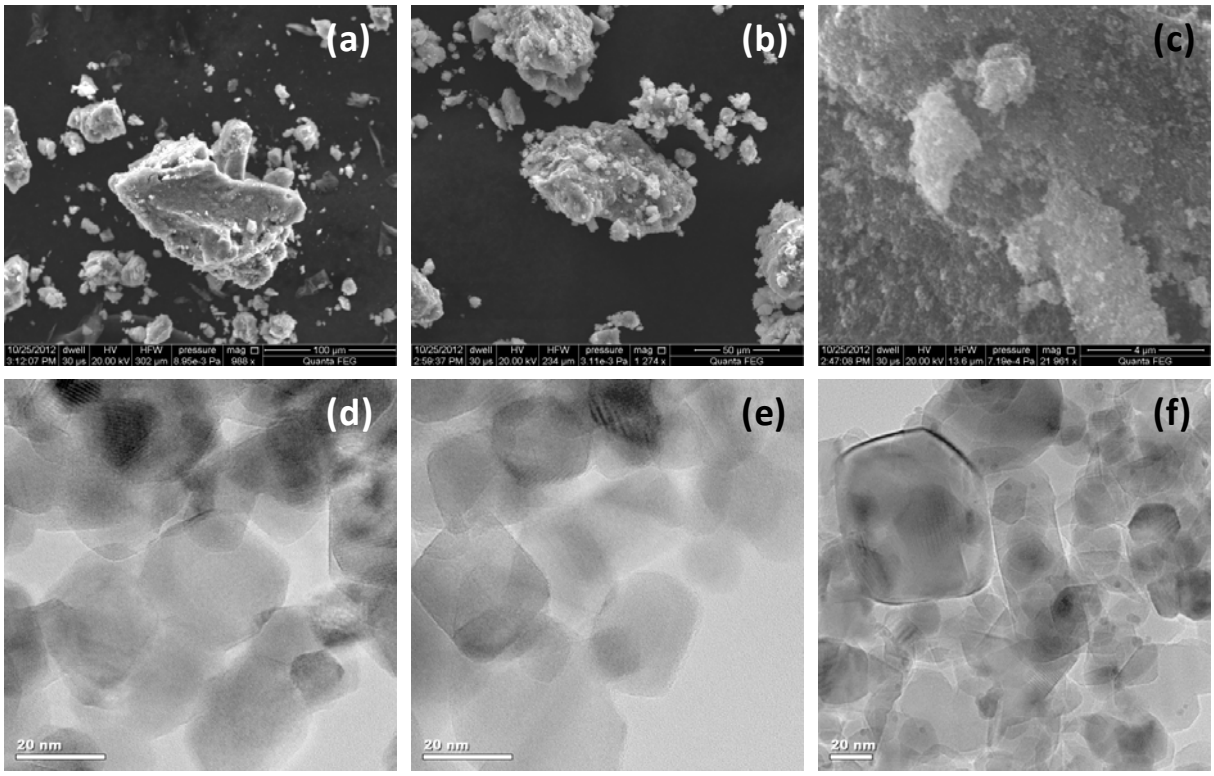

Figure S6. SEM images of (a) Au/TiO_2, (b) Pd/TiO_2, (c) $Au\text{-}Pd/TiO_2$ and TEM images of (d) Au/TiO_2, (e) Pd/TiO_2, (f) $Au\text{-}Pd/TiO_2$

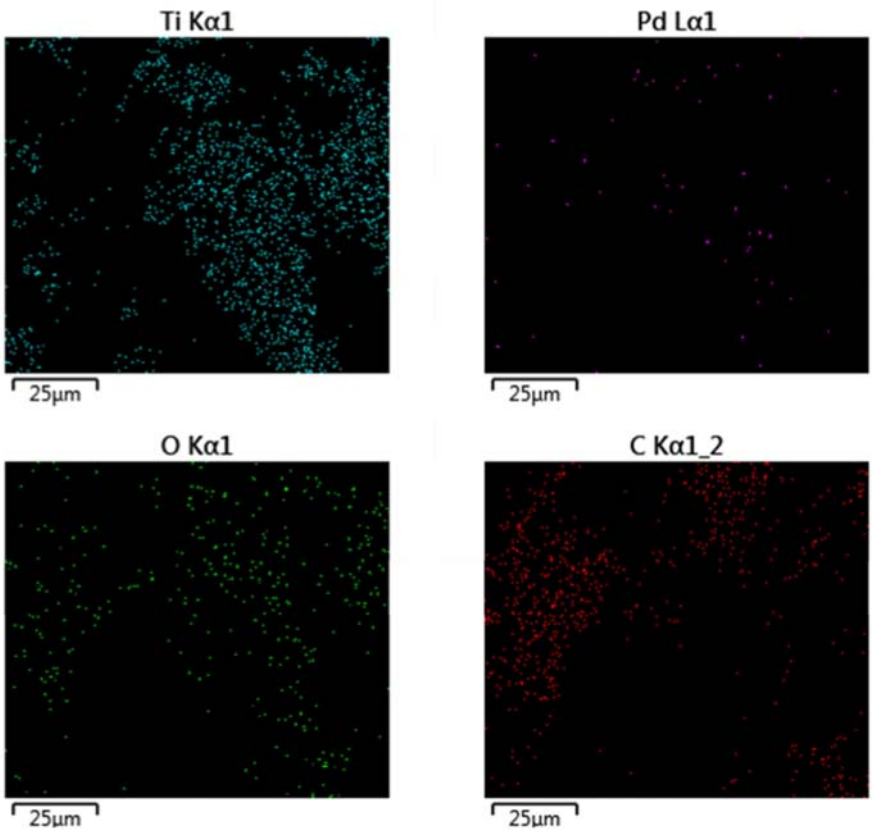

Figure S7. SEM EDS Mapping of Pd/TiO_2 catalyst

Table S1.

Carbonaceous species adsorbed on the catalyst surface

Catalyst	Desorption Temperature (°C)	Carbonaceous species, Weight %
TiO_2 P25 with Oxygen	285	33.6
0.5wt%Pd/TiO_2 with Oxygen	300	47.9
0.5wt%Pd/TiO_2 with less UV light	314	78.1